THE JOURNAL OF PHYSICAL CHEMISTRY Letters

Letter

pubs.acs.org/JPCL

Charge-Transfer Dynamics of Fluorescent Dye-Sensitized Electrodes under Applied Biases

Robert Godin,[†] Benjamin D. Sherman,[§] Jesse J. Bergkamp,[§] Carlos A. Chesta,[‡] Ana L. Moore,[§] Thomas A. Moore,[§] Rodrigo E. Palacios,*[,‡] and Gonzalo Cosa*[,†]

[†]Department of Chemistry and Center for Self-Assembled Chemical Structures (CSACS/CRMAA), McGill University, 801 Sherbrooke Street West, Montreal, Quebec H3A 0B8, Canada

[‡]Departamento de Química, Facultad de Ciencias Exactas Físico-Químicas y Naturales, Universidad Nacional de Río Cuarto, Río Cuarto, Córdoba Argentina

[§]Department of Chemistry and Biochemistry, Center for Bioenergy and Photosynthesis, Arizona State University, Tempe, Arizona 85287-1604, United States

Supporting Information

ABSTRACT: The development of dye-sensitized solar cells requires an in-depth understanding of the interfacial charge-transfer dynamics that take place between dye sensitizers and semiconductors. Here, we describe a prototype system to probe these dynamics by monitoring in real time the fluorescence of two organic sensitizers, a perylene and a squaraine, bound to a SnO_2 semiconductor thin film as a function of potentiostatic control of the Fermi level. The two different sensitizer fluorophores characterized by vastly different redox potentials undergo similar fluorescence modulation with applied bias, an indication that the density of states of the semiconductor largely influences the charge-transfer dynamics while energetics play a minimal role. We further show that the rate of photodegradation of the perylene sensitizer with applied bias provides a suitable marker to study the rate of charge injection and charge recombination. Taken together, our results demonstrate a suitable platform to visualize and study charge-transfer dynamics on films and constitute a step toward achieving single-molecule resolution in our quest to decipher the static and dynamic heterogeneity of charge-transfer dynamics in dye-sensitized photoanodes.

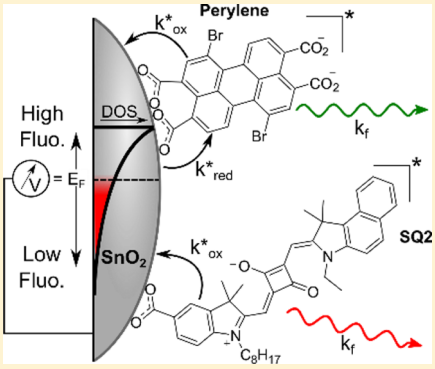

Dye-sensitized solar cells (DSSCs)[1,2] have tremendous potential as a low-cost, easy to manufacture solution to the world's growing energy demands. The dynamics of interfacial charge transfers play a key role in determining how charges flow in the cell and ultimately the power conversion efficiency of DSSCs. Significant advances have been made toward maximizing the efficiency of DSSCs by studying, via transient absorption spectroscopy, the influence of applied biases on rates of electron injection and charge recombination. By monitoring the absorption of the photooxidized sensitizer and that of the injected electron over time, it has been shown that when the Fermi level (E_F) of the semiconductor is raised by applying a negative potential, electronic states are filled, leading to a high density of electrons.[3] The increase in electronic density in turn hampers device performance by both inhibiting electron injection into the semiconductor and accelerating charge recombination with the photooxidized sensitizer.[4−7] The applied bias dependence of charge-transfer pathways are important considerations for the working conditions of DSSCs under sunlight irradiation.[8]

Here, we report the use of fluorescence spectroscopy to probe interfacial charge-transfer dynamics under applied bias. Originally introduced in seminal work by Kamat et al. using MLCT emission rather than fluorescence,[9] the method enables monitoring charge-transfer dynamics from the photoexcited sensitizer as it competes with radiative emission.[10] Fluorescence provides an internal clock of relevant time scales for interfacial charge dynamics, that of the excited-state lifetime dictated by the interplay of radiative decay (ps−ns) and charge transfer. Furthermore, fluorescence boasts unsurpassed sensitivity, reaching single-molecule levels.[11]

In order to study the interfacial charge-transfer dynamics between dyes and metal oxide semiconductors,[12,13] we resorted to a single-molecule/particle spectroelectrochemistry (SMS-EC)[14] setup based on a total internal reflection fluorescence microscope (TIRFM); see Figure 1 and the Supporting Information (SI) for experimental details. The setup enabled photoexcitation at the dye−semiconductor interface by an evanescent field that only penetrates a few hundred nanometers in the solution, spatially excluding fluorescence contributions from dyes that potentially desorb from the semiconductor surface under negative applied bias.[15] We separately monitored the fluorescence of two different organic sensitizers, either a

Received: May 21, 2015
Accepted: June 22, 2015

DOI: 10.1021/acs.jpclett.5b01061
J. Phys. Chem. Lett. 2015, 6, 2688−2693

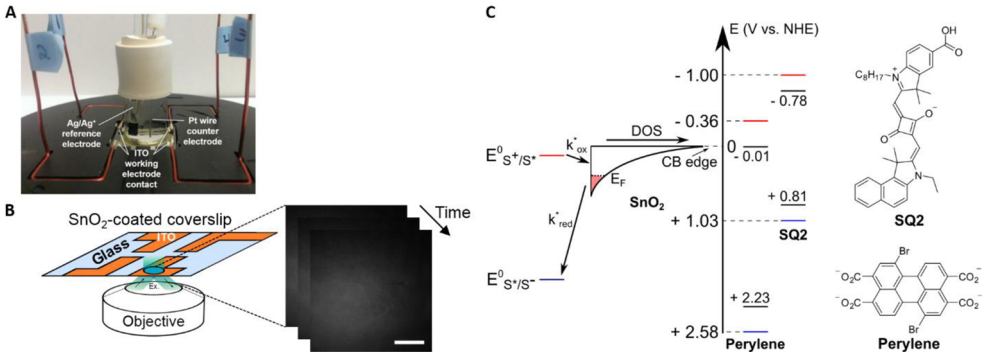

Figure 1. SMS-EC setup. (A) Photograph of the SMS-EC cell illustrating the electrodes and leads for the electrochemical chamber. (B) Cartoon showing the coverslip with four independent L-shaped ITO electrodes and the evanescent optical excitation. Shown to the right is a series of frames from a movie acquired on a perylene-sensitized region of the SnO_2 film under an applied bias of 0.83 V versus NHE. The scale bar is 20 μm. (C) Energy diagram showing the relevant energy levels of the SnO_2 and dyes (chemical structures of the dyes are also shown). Occupied electronic states of the SnO_2 are highlighted in red. The ground-state redox potentials (drawn in black, closed form of the perylene) and the excited-state redox potentials (excited-state oxidation in red and excited-state reduction in blue) are calculated taking into account the E_{00} energies of the sensitizers (opened form for the perylene). To the left is an example of the sensitizer dye (S) photooxidation (k^*_{ox}) and photoreduction (k^*_{red}) pathways.

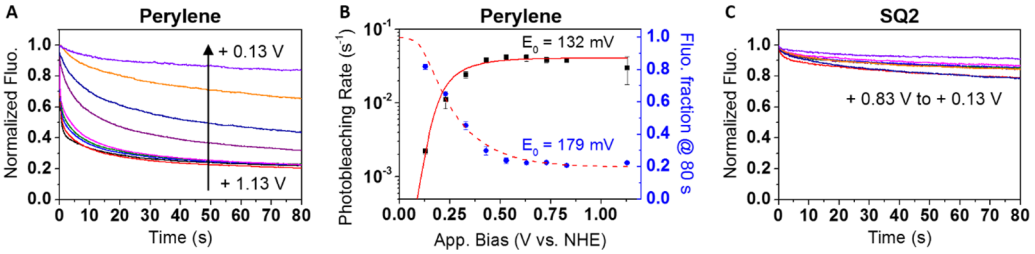

Figure 2. Influence of applied bias on the photobleaching of the fluorescent sensitizer dyes under study. Shown are the normalized fluorescence intensity trajectories of the perylene (A) and SQ2 (C) dyes. (B) Photobleaching rates obtained from stretched exponential fits to the data in (A) and residual fluorescence after 80 s of illumination for the perylene (eqs S1 and S2, SI). The red lines represent fits to the sigmoidal expressions of eqs 1 and 2 below. The best-fit parameters for the energetic distribution of the electronic states (E_0) are noted in the plot. See the SI for experimental and fitting details.

perylene or a squaraine (SQ2), bound to a SnO_2 semiconductor thin film (~35 nm thick, Figure S1 (SI)) under potentiostatic control of the electron density and E_F. These two sensitizers were chosen because their redox potentials are significantly different (Figure 1), allowing for the investigation of the effects of the sensitizer energetics.

We initially compared the fluorescence from the two dyes when no external bias was applied. Images acquired in the microscopy setup show smooth fluorescence profiles, indicating homogeneous surface coverage for both dyes. In the absence of external bias, an open-circuit potential of ~0.4 V (versus NHE) was measured, and we observed fast photobleaching (vide infra) of the perylene fluorescence; however, SQ2 emission was stable over time. Under control of the applied bias (E_{app}) and thus of the E_F of SnO_2, the fluorescence of the perylene dye decayed very rapidly upon illumination at $E_{app} \approx 1$ V. Applying a positive potential decreases the electron density present in the semiconductor film. Qualitatively, the rate of perylene photobleaching decreased significantly with decreasing E_{app} (Figure 2A). SQ2 on the other hand showed limited, bias-independent photobleaching (Figure 2C). Control experiments of perylene bound to a SiO_2 redox-inactive support showed minimal photobleaching (Figure S3, SI). The photobleaching of the perylene in the absence of charge transfer was thus insignificant. Similar results and conclusions were obtained for SQ2 bound to SiO_2.

These initial results highlight the rapid photodegradation of the perylene dye following formation of its radical cation (perylene$^{\bullet+}$) subsequent to electron injection into the SnO_2 (photoinduced oxidation (k^*_{ox}); see also Figure 1 and Schemes S1 and S2 (SI)). The perylene dye used in this work has been shown to inject electrons into TiO_2 nanoparticles (NPs).[16] It is thus also expected to inject electrons into SnO_2, characterized by a conduction band edge (CBE $\approx$ 0 V versus NHE)[9] positively shifted by 0.5 V compared to TiO_2 (CBE ≈ -0.5 V versus NHE).[17] The previously reported irreversible electrochemical oxidation[16] of the perylene supports the rapid transformation of the newly formed perylene$^{\bullet+}$ to nonemissive dark products (Scheme S2, SI). The rate-limiting step of photobleaching is proposed to be the photooxidation of the perylene (k^*_{ox}). Given the excited-state oxidation potentials of perylene and SQ2 and the fact that SQ2 is used in high-performance TiO_2-based DSSCs,[18] photoinduced oxidation should also readily occur for SQ2 on SnO_2 to yield its radical cation (SQ2$^{\bullet+}$). The relatively minor and bias-independent photobleaching observed for SQ2 on SnO_2 supports the high stability of SQ2$^{\bullet+}$, as observed from repeated electrochemical cyclic voltammetry (CV) experiments of SQ2 in solution.[18]

We next extracted from the data in Figure 2A the rates of photobleaching for the perylene dye in order to correlate them to E_{app} and thus obtain the dependence of k^*_{ox} on E_{app}. The rates were quantified by fitting the fluorescence decay trajectories to a stretched exponential expression (see the SI). The perylene photobleaching rates (proportional to k^*_{ox})[19] obtained from the fitted average fluorescence decay rates according to eq S2 (SI) showed a sigmoidal dependence with E_{app} (Figure 2B). A

DOI: 10.1021/acs.jpclett.5b01061
J. Phys. Chem. Lett. 2015, 6, 2688−2693

similar dependence with bias was observed when the fraction of fluorescence remaining after 80 s of illumination ($I_{80\ s}$) at a constant E_{app} was used as the quantitative metric of photobleaching. Equations 1 and 2 provided good fits to the dependence of the rate of photobleaching (and therefore the rate-limiting k_{ox}^{*} under the assumption made in Scheme S2, SI) and $I_{80\ s}$ with E_{app}, respectively.

$$k_{ox}^{*} \propto \text{rate}_{bl} = \text{rate}_{max} \times \int_{\infty}^{\text{Edge}} \left(1 - \frac{1}{1 + \exp\left(\frac{E - E_{app}}{E_0}\right)}\right) \exp\left(-\frac{E}{E_0}\right) dE \quad (1)$$

$$I_{80\ s} = 1 - I_{\text{bleach max}} \times \int_{\infty}^{\text{Edge}} \left(1 - \frac{1}{1 + \exp\left(\frac{E - E_{app}}{E_0}\right)}\right) \times \exp\left(-\frac{E}{E_0}\right) dE \quad (2)$$

In order to interpret eqs 1 and 2, it is important to recall that the interfacial charge-transfer rate between sensitizers and a semiconductor has been shown to depend on an electronic coupling term (V^2), a Fermi–Dirac term to account for the electronic occupancy, a density of states (DOS) term for the semiconductor, and finally an energetic term described by the Marcus–Gerischer theory, shown in going from left to right in eqs 3 and 4.[20] The DOS of metal oxide semiconductors such as TiO_2 and SnO_2 is usually characterized by an exponential tail of states acting as trap sites (with an energetic distribution of E_0) below the conduction band edge, accounting for the $\exp(-E/E_0)$ term.[7,20,21] We conducted chronoamperometry and CV experiments in order to experimentally verify the shape of the DOS of the SnO_2 used in our studies; our data confirmed the energetic exponential dependence of the semiconductor DOS (Figure S6, SI).

$$k_{ox}^{*} = A \int V^2 \times \left(1 - \frac{1}{1 + \exp\left(\frac{E - E_F}{k_B T}\right)}\right) \times \exp\left(-\frac{E}{E_0}\right) \times \exp\left(-\frac{(E - E_{ox}^{*} + \lambda)^2}{4\lambda k_B T}\right) dE \quad (3)$$

$$k_{red}^{*} = A \int V^2 \times \frac{1}{1 + \exp\left(\frac{E - E_F}{k_B T}\right)} \times \exp\left(-\frac{E}{E_0}\right) \times \exp\left(-\frac{(E - E_{red}^{*} - \lambda)^2}{4\lambda k_B T}\right) dE \quad (4)$$

Equations 1 and 2 take into account an exponentially dependent DOS term, where E_0 represents the energetic distribution of the electronic states. Although energetic contributions (Marcus-type dependence of the electron-transfer rate on the free-energy change) cannot be conclusively ruled out, our data consistently show the DOS of the SnO_2 as the dominant factor that controls the changes in rate of interfacial charge transfers. The DOS E_0's extracted from the photobleaching fits are ~130–180 mV, and similar values have been reported for the much more studied TiO_2.[20,22] More importantly, the fitting results are in line with the E_0 values of 90–130 mV obtained from electrochemical measurements of a thick SnO_2 film cast from a 15 wt % SnO_2 NP dispersion (Figure S6, SI). The edge parameter found in eqs 1 and 2 may be physically linked to the approximate upper energies of states that are both active in the charge transfers and whose occupancy is influenced by the changes in E_{app}. Edge values of 0.11–0.15 V are extracted from the fits shown in Figure 2B.

In order to determine the fate of electrons injected into the semiconductor, we measured the photocurrents produced upon photoexcitation of the sensitizers bound to SnO_2 films. Under a constant applied bias of 0.43 V, a larger photocurrent was produced when exciting the perylene over SQ2 despite the lower photon flux used to excite the former versus the latter (Figure 3). These results are rationalized considering that a

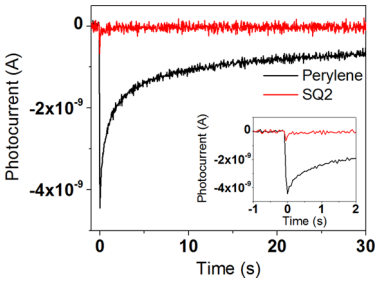

Figure 3. Comparison of the photocurrent measured upon excitation of perylene and SQ2 bound to SnO_2. Laser excitation was initiated at time t = 0 s. The applied bias was kept at 0.43 V before and during irradiation. (Inset) Expanded view of the first 2 s of the photocurrent decay.

significant fraction of the electrons photoinjected into SnO_2 may not recombine with perylene$^{\bullet+}$, presumably due to its rapid degradation. These electrons thus diffuse away from the interface and are efficiently collected at the ITO back contact, giving rise to the observed photocurrent. Considering the charge collected upon irradiation of the perylene and the size of the area illuminated (~150 × 150 μm^2), we estimate ~10 dyes/nm^2 of geometrical area, in line with the expected coverage of a dye monolayer and the rough surface of the SnO_2 layer (Figure S1, SI). In the case of SQ2, we attribute the lower measured photocurrent to an efficient electron–SQ2$^{\bullet+}$ recombination pathway.

Importantly, for perylene-sensitized electrodes, a reduction in the photocurrent magnitude is observed for E_{app} < 0.43 V (Figure S8, SI). Two possible scenarios both related to the higher electron density in SnO_2 may account for this observation; (i) the photooxidation rate of the dye (k_{ox}^{*}) becomes smaller with more negative bias[9,23] and/or (ii) there is a faster recombination between electrons and perylene$^{\bullet+}$, effectively competing with the degradation of the dye.[8]

To distinguish between the two scenarios, we studied the effect of the applied bias on the initial fluorescence intensity (I_0) with our SMS-EC setup (Figure 4). By only taking into account the initial fluorescence intensity, we minimize the effect of bias-dependent photobleaching rates (vide supra). In agreement with the first hypothesis, our studies showed that for perylene (and also SQ2), fluorescence enhancements are recorded at negative biases, the result of suppressed electron injection into the semiconductor in favor of emission. The I_0 thus increased with a lowering of E_{app}, consistent with the reduction of k_{ox}^{*} at more negative biases. The I_0 analysis, however, is insensitive to changes in recombination rates

DOI: 10.1021/acs.jpclett.5b01061
J. Phys. Chem. Lett. 2015, 6, 2688–2693

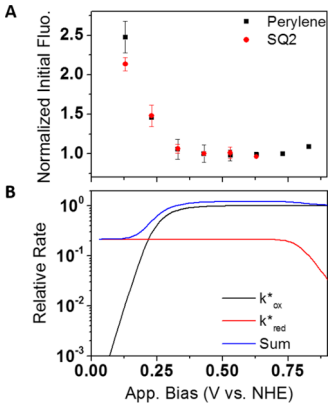

Figure 4. Influence of applied bias on the initial fluorescence intensity of the perylene and SQ2 dyes. (A) Initial fluorescence intensity of both dyes, normalized to the values obtained at 0.43 V. (B) Charge-transfer rate constants relative to the maximal value of k^{*}_{ox} for the perylene as calculated from the fit parameters obtained from Figure S7 (SI).

between electrons and perylene$^{\bullet+}$; therefore, we may not determine whether those processes are occurring, to what extent they are occurring, and how their rate may be affected by the applied potentials. Nonetheless, it is likely that the recombination rates mirror the observed retardation of photoreduction of the perylene with increasing applied bias (vide infra).

Further inspection of the changes in I_0 with E_{app} show a striking similarity in the data recorded for both the perylene and SQ2 compounds (Figure 4A). Given the large difference in the excited-state redox potentials of both dyes (Figure 1), the observed trends indicate that it is highly unlikely that energetics are playing a significant role in dictating the *changes* in rates of charge transfer in our system. Rather, the occupancy of the electronic states of SnO_2 seems to be the dominant factor, in agreement with the above results from photobleaching studies of perylene. Fitting of the I_0 versus E_{app} experimental data retrieved E_0 values between 50 and 90 mV (see the SI for details), similar to those obtained from the analysis of photobleaching and also from the electrochemical characterization.

Figure 4A also reveals that for perylene-sensitized electrodes, the I_0 values increased in going from 0.63 to 0.83 V [no data were available for SQ2 as thermal oxidation takes place at these biases (E^{0}_{ox} = 0.81 V)].[18] To account for this observation with perylene, one must consider a decrease in k^{*}_{red} resulting from a depletion of electrons occupying the electronic states of SnO_2 at increasing positive bias. On the contrary, k^{*}_{ox} would be expected to increase as a result of the decreasing electron density, which would result in the inverse trend, that is, lowering of I_0 with increasing applied bias (Figure 4B).

The above result suggests that photoinduced reduction of a dye (electron transfer from the semiconductor to the photoexcited sensitizer) may take place in operating DSSCs. The efficiency of DSSCs has long been known to be hampered by recombination, the return of an electron injected into SnO_2 to an oxidized dye. Photoinduced reduction, however, has been frequently overlooked when studying the charge-transfer dynamics of DSSCs. Our results point to a contribution arising from photoinduced reduction toward lower power conversion efficiency of a DSSC. The electron density (E_F) in SnO_2 is typically high under operating conditions ($E_F \approx -0.3$ V for $V_{OC} \approx 0.5$ V with the I^-/I_3^- redox mediator), potentially exacerbating the nonproductive k^{*}_{red} process under solar cell working conditions. We believe that sensitizer photoreduction pathways warrant consideration in future solar cell designs.

In closing, we propose a molecular description to rationalize the observations indicating that it is highly unlikely that energetics are playing a significant role in dictating the changes in rates of charge transfer in our system. We note that the bias range explored herein covers only states of SnO_2 found in lower energies compared to the conduction band. States within the band gap for TiO_2 have been associated with surface defects such as undercoordinated Ti atoms or grain boundries.[24−26] Considering the potentially well-defined structure of these states, it seems reasonable to consider that these states are individually fixed in terms of energy.[27] Therefore, the driving force for electron transfer between the localized energy state of the semiconductor and the molecular orbital of the dye sensitizers will be, for the most part, independent of the E_F of the SnO_2. Instead, the occupancy of the electronic state will dictate whether electron transfer is fast/possible (empty accepting state) or slow/inhibited (filled accepting state), in line with single-molecule studies that have shown stochastic fluctuations in electron-transfer rates.[28−30] We envisage that single-molecule spectroelectrochemical studies will provide novel insights in determining the nature of semiconductor energy states that participate in charge transfer.

In summary, both photobleaching and the initial fluorescence intensity analyses indicated that the occupancy of the electronic states of the SnO_2 film dictates the dependence of charge-transfer rates on the applied potential. Previous reports have shown the influence of both DOS[7,8,10] and energetics effects[23,31,32] (or lack of energetic effects[33,34]) on charge-transfer pathways.[35] Our analyses indicate that the DOS of the SnO_2 film dominated over energetic Marcus-type effects in our system, underlining the complex nature of interfacial charge transfers and our limited understanding of the matter.

■ ASSOCIATED CONTENT

Supporting Information

Experimental methods; AFM and electrochemical characterization of the SnO_2 film; controls of sensitizers bound to ITO and SiO_2 surfaces; photobleaching analysis and fits; initial fluorescence intensity fits; perylene photocurrents. The Supporting Information is available free of charge on the ACS Publications website at DOI: 10.1021/acs.jpclett.5b01061.

■ AUTHOR INFORMATION

Corresponding Authors

*E-mail: rpalacios@exa.unrc.edu.ar (R.E.P.).
*E-mail: gonzalo.cosa@mcgill.ca (G.C.).

Notes

The authors declare no competing financial interest.

■ ACKNOWLEDGMENTS

We thank Dr. Ramkaran from the CSACS SPM facility for help with the AFM measurements. G.C. is grateful to the NSERC Canada, a Tomlinson award from McGill University, and CFI for funding. R.G. is thankful to NSERC for a postgraduate scholarship. This work has been supported in part by grants from ANPCyT, Argentina (2691/11, 1439/13, and PRH23 PME01); CONICET, Argentina (PIP 11220100100284/11, and CIAM/09); SeCyT-UNRC, Argentina; MinCyT Cordoba, Argentina (PID 033/2010); NSF, U.S.A., DMR-0908656

DOI: 10.1021/acs.jpclett.5b01061
J. Phys. Chem. Lett. 2015, 6, 2688−2693

(synthetic studies); the Office of Basic Energy Sciences, Division of Chemical Sciences, Geosciences, and Energy Biosciences; DOE under Contract DE-FG02-03ER15393; and the Center for Bio-Inspired Solar Fuel Production, an Energy Frontier Research Center funded by the U.S. DOE, Office of Science, Office of Basic Energy Sciences under Award Number DE-SC0001016. R.E.P. is permanent research staff of CONICET.

REFERENCES

(1) O'Regan, B.; Grätzel, M. A Low-Cost, High-Efficiency Solar-Cell Based on Dye-Sensitized Colloidal TiO_2 Films. *Nature* **1991**, *353*, 737−740.

(2) Yella, A.; Lee, H.-W.; Tsao, H. N.; Yi, C.; Chandiran, A. K.; Nazeeruddin, M. K.; Diau, E. W.-G.; Yeh, C.-Y.; Zakeeruddin, S. M.; Grätzel, M. Porphyrin-Sensitized Solar Cells with Cobalt (II/III)-Based Redox Electrolyte Exceed 12% Efficiency. *Science* **2011**, *334*, 629−634.

(3) Nelson, J.; Haque, S. A.; Klug, D. R.; Durrant, J. R. Trap-Limited Recombination in Dye-Sensitized Nanocrystalline Metal Oxide Electrodes. *Phys. Review. B* **2001**, *63*, 205321.

(4) Willis, R. L.; Olson, C.; O'Regan, B.; Lutz, T.; Nelson, J.; Durrant, J. R. Electron Dynamics in Nanocrystalline ZnO and TiO_2 Films Probed by Potential Step Chronoamperometry and Transient Absorption Spectroscopy. *J. Phys. Chem. B* **2002**, *106*, 7605−7613.

(5) Durrant, J. R. Modulating Interfacial Electron Transfer Dynamics in Dye Sensitised Nanocrystalline Metal Oxide Films. *J. Photochem. Photobiol., A* **2002**, *148*, 5−10.

(6) Green, A. N. M.; Palomares, E.; Haque, S. A.; Kroon, J. M.; Durrant, J. R. Charge Transport versus Recombination in Dye-Sensitized Solar Cells Employing Nanocrystalline TiO_2 and SnO_2 Films. *J. Phys. Chem. B* **2005**, *109*, 12525−12533.

(7) Knauf, R. R.; Brennaman, M. K.; Alibabaei, L.; Norris, M. R.; Dempsey, J. L. Revealing the Relationship between Semiconductor Electronic Structure and Electron Transfer Dynamics at Metal Oxide−Chromophore Interfaces. *J. Phys. Chem. C* **2013**, *117*, 25259−25268.

(8) Haque, S. A.; Tachibana, Y.; Willis, R. L.; Moser, J. E.; Grätzel, M.; Klug, D. R.; Durrant, J. R. Parameters Influencing Charge Recombination Kinetics in Dye-Sensitized Nanocrystalline Titanium Dioxide Films. *J. Phys. Chem. B* **2000**, *104*, 538−547.

(9) Kamat, P. V.; Bedja, I.; Hotchandani, S.; Patterson, L. K. Photosensitization of Nanocrystalline Semiconductor Films. Modulation of Electron Transfer between Excited Ruthenium Complex and SnO_2 Nanocrystallites with an Externally Applied Bias. *J. Phys. Chem.* **1996**, *100*, 4900−4908.

(10) McNeil, I. J.; Alibabaei, L.; Ashford, D. L.; Fecko, C. J. Investigation of Factors That Affect Excited-State Lifetime Distribution of Dye-Sensitized Nanoparticle Films. *J. Phys. Chem. C* **2013**, *117*, 17412−17420.

(11) Hill, C. M.; Clayton, D. A.; Pan, S. Combined Optical and Electrochemical Methods for Studying Electrochemistry at the Single Molecule and Single Particle Level: Recent Progress and Perspectives. *Phys. Chem. Chem. Phys.* **2013**, *15*, 20797−20807.

(12) Reeja-Jayan, B.; Adachi, T.; Ono, R. J.; Vanden Bout, D. A.; Bielawski, C. W.; Manthiram, A. Effect of Interfacial Dipoles on Charge Traps in Organic−Inorganic Hybrid Solar Cells. *J. Mater. Chem. A* **2013**, *1*, 3258−3262.

(13) Reeja-Jayan, B.; Koen, K. A.; Ono, R. J.; Vanden Bout, D. A.; Bielawski, C. W.; Manthiram, A. Oligomeric Interface Modifiers in Hybrid Polymer Solar Cell Prototypes Investigated by Fluorescence Voltage Spectroscopy. *Phys. Chem. Chem. Phys.* **2015**, *17*, 10640−10647.

(14) Palacios, R. E.; Fan, F.-R. F.; Bard, A. J.; Barbara, P. F. Single-Molecule Spectroelectrochemistry (SMS-EC). *J. Am. Chem. Soc.* **2006**, *128*, 9028−9029.

(15) Lemon, B. I.; Hupp, J. T. EQCM Investigations of Dye-Functionalized Nanocrystalline Titanium Dioxide Electrode/Solution Interfaces: Does Luminescence Report Directly on Interfacial Electron Transfer Kinetics? *J. Phys. Chem. B* **1999**, *103*, 3797−3799.

(16) Hernández, L. I.; et al. Spectral Characteristics and Photosensitization of TiO_2 Nanoparticles in Reverse Micelles by Perylenes. *J. Phys. Chem. B* **2012**, *117*, 4568−4581.

(17) Asbury, J. B.; Hao, E.; Wang, Y.; Ghosh, H. N.; Lian, T. Ultrafast Electron Transfer Dynamics from Molecular Adsorbates to Semiconductor Nanocrystalline Thin Films. *J. Phys. Chem. B* **2001**, *105*, 4545−4557.

(18) Geiger, T.; Kuster, S.; Yum, J.-H.; Moon, S.-J.; Nazeeruddin, M. K.; Grätzel, M.; Nüesch, F. Molecular Design of Unsymmetrical Squaraine Dyes for High Efficiency Conversion of Low Energy Photons into Electrons Using TiO_2 Nanocrystalline Films. *Adv. Funct. Mater.* **2009**, *19*, 2720−2727.

(19) The observed rate of photobleaching is linked to the rate constant k_{ox}^{*} through the concentration of excited dye, itself dependent on the excitation rate, the quantum yield of photooxidation. Without access to these parameters, we limit ourselves to the changes in rates under varying E_{app}.

(20) Listorti, A.; O'Regan, B.; Durrant, J. R. Electron Transfer Dynamics in Dye-Sensitized Solar Cells. *Chem. Mater.* **2011**, *23*, 3381−3399.

(21) Ardo, S.; Meyer, G. J. Photodriven Heterogeneous Charge Transfer with Transition-Metal Compounds Anchored to TiO_2 Semiconductor Surfaces. *Chem. Soc. Rev.* **2009**, *38*, 115−164.

(22) Bailes, M.; Cameron, P. J.; Lobato, K.; Peter, L. M. Determination of the Density and Energetic Distribution of Electron Traps in Dye-Sensitized Nanocrystalline Solar Cells. *J. Phys. Chem. B* **2005**, *109*, 15429−15435.

(23) Tachibana, Y.; Haque, S. A.; Mercer, I. P.; Moser, J. E.; Klug, D. R.; Durrant, J. R. Modulation of the Rate of Electron Injection in Dye-Sensitized Nanocrystalline TiO_2 Films by Externally Applied Bias. *J. Phys. Chem. B* **2001**, *105*, 7424−7431.

(24) Jankulovska, M.; Berger, T.; Wong, S. S.; Gómez, R.; Lana-Villarreal, T. Trap States in TiO_2 Films Made of Nanowires, Nanotubes or Nanoparticles: An Electrochemical Study. *ChemPhysChem* **2012**, *13*, 3008−3017.

(25) Nunzi, F.; Mosconi, E.; Storchi, L.; Ronca, E.; Selloni, A.; Grätzel, M.; De Angelis, F. Inherent Electronic Trap States in TiO_2 Nanocrystals: Effect of Saturation and Sintering. *Energy Env. Sci.* **2013**, *6*, 1221−1229.

(26) Rittmann-Frank, M. H.; Milne, C. J.; Rittmann, J.; Reinhard, M.; Penfold, T. J.; Chergui, M. Mapping of the Photoinduced Electron Traps in TiO_2 by Picosecond X-ray Absorption Spectroscopy. *Angew. Chem., Int. Ed.* **2014**, *53*, 5858−5862.

(27) McNeil, I. J.; Ashford, D. L.; Luo, H.; Fecko, C. J. Power-Law Kinetics in the Photoluminescence of Dye-Sensitized Nanoparticle Films: Implications for Electron Injection and Charge Transport. *J. Phys. Chem. C* **2012**, *116*, 15888−15899.

(28) Biju, V.; Micic, M.; Hu, D.; Lu, H. P. Intermittent Single-Molecule Interfacial Electron Transfer Dynamics. *J. Am. Chem. Soc.* **2004**, *126*, 9374−9381.

(29) Wong, N. Z.; Ogata, A. F.; Wustholz, K. L. Dispersive Electron-Transfer Kinetics from Single Molecules on TiO_2 Nanoparticle Films. *J. Phys. Chem. C* **2013**, *117*, 21075−21085.

(30) Rao, V. G.; Dhital, B.; He, Y.; Lu, H. P. Single-Molecule Interfacial Electron Transfer Dynamics of Porphyrin on TiO_2 Nanoparticles: Dissecting the Complex Electronic Coupling Dependent Dynamics. *J. Phys. Chem. C* **2014**, *118*, 20209−20221.

(31) Yan, S. G.; Prieskorn, J. S.; Kim, Y.; Hupp, J. T. In Search of the Inverted Region: Chromophore-Based Driving Force Dependence of Interfacial Electron Transfer Reactivity at the Nanocrystalline Titanium Dioxide Semiconductor/Solution Interface. *J. Phys. Chem. B* **2000**, *104*, 10871−10877.

(32) Farnum, B. H.; Morseth, Z. A.; Brennaman, M. K.; Papanikolas, J. M.; Meyer, T. J. Driving Force Dependent, Photoinduced Electron Transfer at Degenerately Doped, Optically Transparent Semiconductor Nanoparticle Interfaces. *J. Am. Chem. Soc.* **2014**, *136*, 15869−15872.

DOI: 10.1021/acs.jpclett.5b01061
J. Phys. Chem. Lett. 2015, 6, 2688−2693

(33) Hasselmann, G. M.; Meyer, G. J. Diffusion-Limited Interfacial Electron Transfer with Large Apparent Driving Forces. *J. Phys. Chem. B* **1999**, *103*, 7671−7675.
(34) Tachibana, Y.; Haque, S. A.; Mercer, I. P.; Durrant, J. R.; Klug, D. R. Electron Injection and Recombination in Dye Sensitized Nanocrystalline Titanium Dioxide Films: A Comparison of Ruthenium Bipyridyl and Porphyrin Sensitizer Dyes. *J. Phys. Chem. B* **2000**, *104*, 1198−1205.
(35) Hagfeldt, A.; Boschloo, G.; Sun, L.; Kloo, L.; Pettersson, H. Dye-Sensitized Solar Cells. *Chem. Rev.* **2010**, *110*, 6595−6663.

DOI: 10.1021/acs.jpclett.5b01061
J. Phys. Chem. Lett. 2015, 6, 2688−2693